Binding energy, structure, and vibrational spectra of $(HCl)_{2-6}$ and $(HF)_{2-10}$ clusters by density functional theory

R. C. Guedes, P. C. do Couto, and B. J. Costa Cabral[a)]
Grupo de Física Matemática da Universidade de Lisboa, Av. Professor Gama Pinto 2, 1649-003 Lisboa, Portugal and Departamento de Química e Bioquímica, Faculdade de Ciências da Universidade de Lisboa, 1749-016 Lisboa, Portugal

(Received 6 September 2002; accepted 22 October 2002)

We are reporting density functional theory results for the binding energies, structures, and vibrational spectra of $(H\text{-}Cl)_{2-6}$ and $(H\text{-}F)_{2-10}$ clusters. The performance of different functionals has been investigated. The properties of HF clusters predicted by hybrid functionals are in good agreement with experimental information. The HCl dimer binding energy ΔE_e is underestimated by hybrid functionals. The Perdew and Wang exchange and correlation functional (PW91) result for ΔE_e is $-9.6\ \mathrm{kJ\,mol^{-1}}$, in very good agreement with experiment ($-9.5\ \mathrm{kJ\,mol^{-1}}$). However, PW91 overestimates binding energies of larger clusters. Hydrogen bonding cooperativity depends on the cluster size n but reaches a limit for moderately sized clusters ($n=8$ for HF). The average shift to low frequencies ($\Delta\nu$) of the X-H ($X=$Cl,F) stretching vibration relative to the monomer is in good agreement with experimental data for HF clusters in solid neon. However, some discrepancies with experimental results for HCl clusters were observed. The behavior of $\Delta\nu$ as a function of the cluster size provides an interesting illustration of hydrogen-bond cooperative effects on the vibrational spectrum. The representation of the electronic density difference shows the rearrangement of the electronic density induced by hydrogen bonding in the clusters and supports the view that hydrogen-bond cooperativity is related to electronic sharing and delocalization. © *2003 American Institute of Physics.* [DOI: 10.1063/1.1528952]

I. INTRODUCTION

Clusters of hydrogen-bonded molecules are extremely important as model systems in the study of intermolecular interactions and chemical reactivity.[1,2] One particularly relevant aspect of these aggregates is hydrogen-bonding cooperativity. This means that due the nonadditive character of the polarization effects involved in hydrogen bonding, the structure and energetics of the aggregates are very dependent on the size of the system. One important issue concerns the dependence of structural and electronic properties on the number of monomers in the cluster (n) or cluster size and the possible extrapolations to larger clusters. This must rely on the expectation that for clusters larger than a size limit n, the importance of these nonadditive effects are significantly reduced. The study of clusters can be also very useful to understand condensed phase properties. Clusters are structures intermediate between the isolated species and the bulk phases. Thus, it is reasonable to assume that some features of condensed phases are already present in the aggregates.

The nature of hydrogen bonding is still controversial. Charge transfer,[3] electrostatic effects,[4,5] and more recently, partial covalent contributions[6] have been invoked to explain the structure and binding energies in hydrogen-bonding systems. One specific aspect of hydrogen bonding concerns the relative importance of different contributions to the interaction energy. Thus, for hydrogen chloride it is expected that dispersion interactions are the dominating contribution to the intermolecular interactions.[7,8] This feature is different from the well-known role played by electrostatic interactions in classical hydrogen-bonded systems, as, for example, water, and hydrogen fluoride.

Several experimental[9–19] and theoretical studies[7,8,20–24] for the HCl dimer have been reported. Theoretical studies for larger HCl clusters are still relatively scarce. Latajka and Scheiner analyzed the structure, energetics and vibrational spectra of dimers, trimers and tetramers of HX ($X=$Cl,Br,I).[8] Chandler *et al.* studied reactions involving hydrogen halides polymers and optimized $(HCl)_{1-4}$ clusters at the second-order Møller–Plesset (MP2) theoretical level.[25]

Numerous works on HF clusters have been carried out including experimental investigations[10,26–30] and theoretical calculations.[24,31–39] Extensive compilation of thermodynamical data including enthalpies and entropies of HF clusters[37] have been published.

An important aspect characterizing hydrogen-bonding cooperativity in X-H clusters ($X=$F,Cl,Br,...) is a shift to low frequencies ($\Delta\nu$) and the increase in the intensity of the fundamental X-H stretching vibration relative to the monomer.[1] This aspect has been investigated by several vibrational spectroscopy works on HCl (Refs. 15–19) and HF (Refs. 28–30) clusters. A recent theoretical study[24] analyzed the vibrational properties of HX ($X=$F, Cl, and Br) dimers. However, a theoretical investigation on the vibrational properties of larger clusters seems to be missing still.

In the present work we report a theoretical study of the

a)Author to whom correspondence should be addressed. Electronic address: ben@adonis.cii.fc.ul.pt

TABLE I. Binding energies (in kJ mol^{-1}) for $(HCl)_{2-6}$ clusters. BSSE is the basis set superposition error correction to the electronic binding energy ΔE_e.

	$(HCl)_2$	$(HCl)_3$	$(HCl)_4$	$(HCl)_5$	$(HCl)_6$
B3LYP/aug-cc-pVDZ					
ΔE_0	−1.9	−10.2	−20.8	−26.6	−31.9
$\Delta E_{0,n,n-1}$	−1.9	−8.3	−10.5	−5.8	−5.3
ΔE_e	−6.2	−21.4	−37.5	−47.9	−57.9
BSSE	0.7	1.9	3.4	4.4	5.4
$\Delta E_{e,n,n-1}$	−6.2	−15.1	−16.1	−10.4	−9.9
B3PLYP/aug-cc-pVTZ					
ΔE_e	−5.5	−19.0	−32.9	−41.9	−50.5
BSSE	0.7	1.9	3.4	4.4	5.4
$\Delta E_{e,n,n-1}$	−5.5	−13.5	−13.9	−9.0	−8.6
B3LYP/aug-cc-pVQZ					
ΔE_e	−5.3	−18.5	−31.9	−40.5	−48.8
BSSE	0.06	0.17	0.29	0.36	
$\Delta E_{e,n,n-1}$	−5.3	−13.2	−13.4	−8.7	−8.2
B3PW91/aug-cc-pVDZ					
ΔE_0	−0.8	−7.7	−17.2	−22.2	−26.7
$\Delta E_{0,n,n-1}$	−0.8	−6.8	−9.6	−5.0	−4.4
ΔE_e	−5.1	−19.0	−34.3	−43.7	−52.9
$\Delta E_{e,n,n-1}$	−5.1	−13.9	−15.3	−9.5	−9.1
MPW1PW91/aug-cc-pVDZ					
ΔE_0	−2.9	−13.6	−26.1		−41.0
$\Delta E_{0,n,n-1}$	−2.9	−10.7	−12.5		
ΔE_e	−7.2	−25.0	−43.2	−54.5[a]	−67.3
$\Delta E_{e,n,n-1}$	−7.2	−17.8	−18.3	−11.3	−12.8
MPW1PW91/aug-cc-pVTZ					
ΔE_e	−6.2	−21.9	−37.7	−47.2	−58.4
$\Delta E_{e,n,n-1}$	−6.2	−15.7	−15.7	−9.6	−11.3
MPW1PW91/aug-cc-pVQZ					
ΔE_e	−5.9	−21.1	−36.1	−45.3	−55.8
$\Delta E_{e,n,n-1}$	−5.9	−15.1	−15.0	−9.2	−10.5
PW91/aug-cc-pVDZ[b]					
ΔE_e	−10.4	−35.5	−61.2	−78.3	−95.3
$\Delta E_{e,n,n-1}$	−10.4	−25.1	−25.6	−17.2	−16.9
PW91/aug-cc-pVTZ[b]					
ΔE_e	−9.7	−32.9	−56.3	−72.0	−87.6
$\Delta E_{e,n,n-1}$	−9.7	−23.2	−23.4	−15.7	−15.5
PW91/aug-cc-pVQZ[b]					
ΔE_e	−9.6	−32.4	−55.3	−70.7	−85.9
$\Delta E_{e,n,n-1}$	−9.6	−22.8	−22.9	−15.4	−15.2
ΔE_0	−2.3;[c] −1.3;[d]				
ΔE_e	−5.9;[e] −6.7;[f] −7.5[g]				
Experiment[h]					
ΔE_0	−5.1				
ΔE_e	−9.5				

[a]Geometry of the pentamer optimized at B3LYP/aug-cc-pVDZ.
[b]Single-point energy calculation with the B3LYP/aug-cc-pVDZ geometry.
[c]MP2/6-311+G($2df,p$) (Ref. 24).
[d]QCISD/6-311+G($2df,p$) (Ref. 24).
[e]MP2/6-31G(d,p) (Ref. 1).
[f]B3LYP/6-31+G(d,p) (Ref. 22).
[g]B3LYP/6-31++G(d,p) (Ref. 22).
[h]From Pine and Howard (Ref. 10).

properties of hydrogen chloride $(HCl)_{2-6}$ and hydrogen fluoride $(HF)_{2-10}$ clusters, which is based on density functional theory. We discuss the energetical, structural, and vibrational properties of the clusters, hydrogen-bond cooperativity, and its dependence on the cluster size. We also analyze the electronic density rearrangement induced by hydrogen bonding through the representation of electronic density difference isosurfaces.

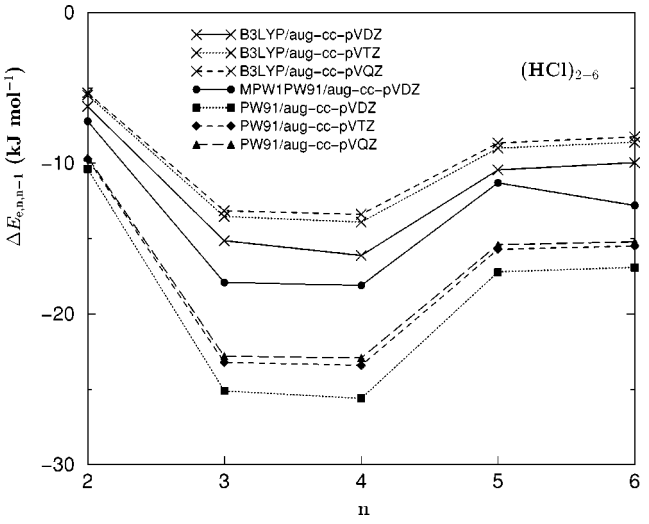

FIG. 1. Stepwise binding energy $\Delta E_{e,n,n-1}$ (in kJ mol^{-1}) vs the cluster size n in $(HCl)_{2-6}$ clusters.

II. COMPUTATIONAL DETAILS

$(HCl)_{2-6}$ and $(HF)_{2-10}$ clusters have been studied at different theoretical levels. Density functional theory (DFT) calculations have been carried out with several hybrid functionals including the Becke three-parameter[40] (B3) with the Perdew and Wang[41] (PW91) and Lee, Yang, and Parr[42] (LYP) correlation functionals. Calculations with the Adamo and Barone[43] Becke style one-parameter functional using a modified Perdew–Wang exchange and PW91 correlation[44,45] (MPW1PW91) have been also carried out. We have also investigated the performance of the Perdew and Wang exchange and correlation functional[41] (PW91) for the prediction of energetic properties of the clusters.

The geometries have been fully optimized with the Dunning's correlation consistent polarized valence double zeta basis set augmented with diffuse functions (aug-cc-pVDZ)[46] and by carrying out frequency calculations the optimized structures have been characterized as local minima. Single-point energies with the triple zeta (aug-cc-pVTZ) and quadruple zeta (aug-cc-pVQZ) basis sets[47] are also reported. The calculations have been carried out with the GAUSSIAN 98 program.[48]

To analyze the energetics of the HF and HCl clusters it is convenient to introduce the binding energy and the stepwise binding energy. The binding energy for a cluster with n monomers $\Delta E_{0,n}$ is defined as

$$\Delta E_{0,n}=E_0[(HX)_n]-nE_0[(HX)], \tag{1}$$

where $X=(F,Cl)$. The stepwise binding energy $\Delta E_{0,n,n-1}$ is given by

$$\Delta E_{0,n,n-1}=E_0[(HX)_n]-E_0[(H)X_{n-1}]-E_0[(HX)]. \tag{2}$$

We also define $\Delta E_{e,n}$ and $\Delta E_{e,n,n-1}$, which are similar to the previously defined quantities but do not include the zero-point vibrational energy (ZPVE) corrections.

B3LYP binding energies were corrected for basis set superposition error (BSSE) by using the counterpoise method[49] including the fragment relaxation energy contributions.[50] We have verified that BSSE corrections to binding energies at the B3LYP/aug-cc-pVQZ level are typically $\sim 1\%$ of the uncorrected values (see Sec. III). For other functionals, binding energies were not corrected. To minimize finite size basis set effects we have carried out single-point energy calculations with the largest affordable basis set for the present systems (aug-cc-pVQZ).

For HF and HCl dimers only the linear structures that contain one hydrogen bond were studied. The cyclic dimers are transition state structures.[8,35] We report results for the cyclic $(HCl)_{3-6}$ and $(HF)_{3-10}$ clusters. There is theoretical[51] and experimental[15] evidence that these structures are more stable than open chains.

III. BINDING ENERGIES AND STRUCTURAL PROPERTIES

A. Binding energies

Binding energies for $(HCl)_{2-6}$ clusters are reported in Table I. Good agreement between our results and other theoretical predictions is observed. For example, ΔE_e from MPW1PW91/aug-cc-pVDZ (-7.2 kJ mol^{-1}) is in excellent agreement with the B3LYP/6-31++G(d,p) value (-7.5 kJ mol^{-1}) reported by Guo *et al.*[22] For B3LYP calculations and some clusters, electronic binding energies (ΔE_e's) were corrected for BSSE and the corrections are reported in Table I. At the B3LYP/aug-cc-pVDZ level BSSE corrections are $\sim 4\%$ of the binding energies. They are reduced to $\sim 1\%$ of the uncorrected values when the calculations are carried out with the larger aug-cc-pVQZ basis set. Our results for the $(HCl)_2$ binding energy based on hybrid functionals are -5.3 kJ mol^{-1} (B3LYP/aug-cc-pVQZ) and -5.9 kJ mol^{-1} (MPW1PW91/aug-cc-pVQZ). The experimental value reported by Pine and Howard[10] is -9.49 ± 1.03 kJ mol^{-1}. For ΔE_0, which includes ZPVE corrections, our best prediction is -2.9 kJ mol^{-1} (MPW1PW91/aug-cc-pVDZ), which is 56% above the experimental value (-5.15 ± 0.26).[10]

Dispersion interactions are expected to contribute significantly to the energetical stabilization of HCl clusters. Thus, the deviation of the $(HCl)_2$ disssociation energy predicted by DFT calculations from the experimental result has been related to the inherent deficiency of DFT methods to describe the energetics of compounds where dispersion interactions are dominant.[24] However, significant deviations from experiment are also observed for ΔE_0's based on MP2 and quadratic configuration interaction including single and double substitutions (QCISD) methods.[24] Recently, Tsuzuki and Lüthi[52] discussed the performance of DFT for the prediction of intermolecular interaction energies of several complexes where dispersion interactions are expected to be important including neon, argon, and hydrogen-bonded complexes. This study suggested that for these systems, the Perdew and Wang exchange and correlation functional[41] (PW91) provided an adequate description of the interaction energies.

Table I also presents binding energies for the HCl clusters based on single-point energy calculations with the PW91 functional. For the HCl clusters PW91 binding energies are

TABLE II. Binding energies (in kJ mol^{-1}) for $(HF)_{2-10}$ clusters. BSSE is the basis set superposition error correction to the electronic binding energy ΔE_e.

	$(HF)_2$	$(HF)_3$	$(HF)_4$	$(HF)_5$	$(HF)_6$	$(HF)_7$	$(HF)_8$	$(HF)_9$	$(HF)_{10}$
B3LYP/aug-cc-pVDZ									
ΔE_0	−11.8	−44.3	−91.5	−129.8	−161.0	−189.6	−218.7	−246.8	−274.6
$\Delta E_{0,n,n-1}$	−11.8	−32.5	−47.2	−38.3	−31.2	−28.6	−29.0	−28.1	−27.8
ΔE_e	−19.3	−65.4	−122.9	−169.0	−207.5	−244.4	−281.4	−317.1	−352.7
BSSE	0.8	3.4	5.3	6.9	8.5	10.1	11.5	12.9	
$\Delta E_{e,n,n-1}$	−19.3	−46.1	−57.5	−46.1	−38.5	−36.9	−37.0	−35.7	−35.7
B3LYP/aug-cc-pVTZ[a]									
ΔE_e	−18.8	−63.7	−121.6	−168.3	−206.8	−243.3	−280.2	−315.8	−351.4
BSSE	0.3	1.0	1.8	2.5	3.0	3.6	4.1	4.6	
$\Delta E_{e,n,n-1}$	−18.8	−44.9	−57.9	−46.6	−38.5	−36.6	−36.9	−35.6	−35.5
B3LYP/aug-cc-pVQZ[a]									
ΔE_e	−18.9	−63.6	−120.9	−166.9	−205.2	−241.4	−278.0	−313.3	−348.6
BSSE	0.17	0.54	0.91	1.24	1.49	1.78			
$\Delta E_{e,n,n-1}$	−18.9	−44.7	−57.3	−46.1	−38.2	−36.3	−36.5	−35.3	−35.3
B3PW91/aug-cc-pVDZ									
ΔE_0	−8.7	−36.7	−80.1	−115.1	−142.8	−168.5	−194.6	−219.6	−244.5
$\Delta E_{0,n,n-1}$	−8.7	−27.9	−43.4	−35.0	−27.8	−25.7	−26.1	−25.0	−24.9
ΔE_e	−16.2	−57.7	−111.2	−154.0	−189.2	−223.0	−256.9	−289.5	−322.1
$\Delta E_{e,n,n-1}$	−16.2	−41.5	−53.6	−42.8	−35.2	−33.7	−34.0	−32.6	−32.6
MPW1PW91/aug-cc-pVDZ									
ΔE_0	−11.2	−43.0	−89.4	−127.3	−157.9	−186.5	−215.0	−242.6	−270.0
$\Delta E_{0,n,n-1}$	−11.2	−31.8	−46.4	−37.9	−30.6	−28.6	−28.4	−27.6	−27.4
ΔE_e	−18.6	−64.1	−120.7	−166.4	−204.5	−240.9	−277.5	−312.8	−347.9
$\Delta E_{e,n,n-1}$	−18.6	−45.5	−56.6	−45.7	−38.0	−36.4	−36.6	−35.3	−35.2
PW91/aug-cc-pVDZ[b]									
ΔE_e	−22.2	−76.9	−143.3	−196.6	−241.0				
$\Delta E_{e,n,n-1}$	−22.2	−54.7	−66.4	−53.2	−44.5				
PW91/aug-cc-pVTZ[b]									
ΔE_e	−21.5	−74.9	−141.3	−194.4	−238.5				
$\Delta E_{e,n,n-1}$	−21.5	−53.4	−66.4	−53.1	−44.1				
PW91/aug-cc-pVQZ[b]									
ΔE_e	−21.4	−74.3	−139.9	−192.4	−236.1				
$\Delta E_{e,n,n-1}$	−21.4	−52.9	−65.6	−52.4	−43.6				
ΔE_0	−11.2[c]								
ΔE_e[d]	−21.3	−69.1	−129.7	−179.6	−221.0	−257.8	−291.5		
				Experiment					
ΔE_e	−19.2[e]								

[a]Single-point energy calculation. Geometry optimized at B3LYP/aug-cc-pVDZ.
[b]Single-point energy calculation with the B3LYP/aug-cc-pVDZ geometry.
[c]B3LYP/6-311+G($2df,p$) (Ref. 24).
[d]B3LYP/6-31++G(d,p) (Ref. 35).
[e]From Pine and Howard (Ref. 10).

significantly lower than the other theoretical methods. For the HCl dimer, ΔE_e calculated at PW91/aug-cc-pVQZ with the geometry optimized at B3LYP/aug-cc-pVDZ is -9.6 kJ mol^{-1}, which is in excellent agreement with experiment.

The importance of cooperative effects due to nonadditive interactions in HCl clusters as a function of the cluster size is illustrated in Fig. 1, which shows the stepwise binding energy $\Delta E_{e,n,n-1}$ as a function of the cluster size n. $\Delta E_{e,n,n-1}$ increases by $\sim$40% from $(HCl)_2$ to $(HCl)_3$, shows a small increase from $(HCl)_3$ to $(HCl)_4$, then decreases and seems to stabilize for larger clusters.

Binding energies for $(HF)_{2-10}$ clusters are reported in Table II. The experimental values for the dimer[10] with and without ZPVE are -12.7 kJ mol^{-1} and -19.4 kJ mol^{-1}, respectively. Our result for the dimer binding energy at the B3LYP/aug-cc-pVQZ level is -18.9 kJ mol^{-1}, which is in good agreement with experiment. By including ZPVE our best estimation is -11.8 kJ mol^{-1}, which indicates that zero-point vibrational energies are reasonably accurate. BSSE for HF clusters are reported in Table II. They are similar to the corrections for HCl binding energies and correspond to $\sim$1% of the uncorrected values at the B3LYP/aug-cc-pVQZ level. PW91 results with geometries optimized at the MPW1PW91/aug-cc-pVDZ level are also reported in Table II. The PW91/aug-cc-pVQZ prediction for the $(HF)_2$ binding energy is -21.4 kJ mol^{-1}, in very good agreement with the result reported by Rincón *et al.*[35] (see Table II) and experiment. Table II also reports binding energies for larger HF clusters. Good agreement between the present results and

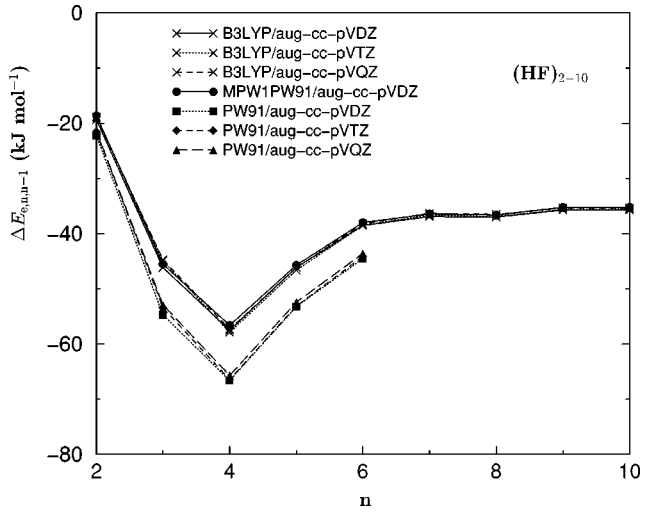

FIG. 2. Stepwise binding energy $\Delta E_{e,n,n-1}$ (in kJ mol^{-1}) vs the cluster size n in $(HF)_{2-10}$ clusters.

other theoretical calculations[35] for clusters up to the octamer is observed. PW91 binding energies for larger clusters are also reported in Table II. They follow the same trend observed in HCl clusters and are significantly lower than those predicted by other theoretical methods.

The most interesting feature concerning binding energy in HF clusters is the strong nonadditive cooperative effect that is observed when we move from the dimer to the trimer and tetramer. This is clearly illustrated in Fig. 2, which presents the stepwise binding energy $\Delta E_{0,n,n-1}$ as a function of n. $\Delta E_{0,n,n-1}$ significantly increases from $n=2$ (dimer) to $n=4$ (tetramer), decreases up to $n=6$ (hexamer), and apparently reaches a plateau for $n \geqslant 8$.

B. Structural properties

The optimized structures of the $(HCl)_{2-6}$ clusters are presented in Fig. 3 and some structural parameters are reported in Table III. The Cl-Cl internuclear distance for $(HCl)_2$ calculated at the MPW1PW91/aug-cc-pVDZ level (3.790 Å) is in excellent agreement with the experimental value reported by Ohashi and Pine (3.797 Å).[9] B3LYP and B3PW91 calculations for the Cl-Cl distance in the dimer deviate from the experimental value by ~0.03 Å. We have verified that the structure of the HCl dimer predicted by the PW91 functional is not in good agreement with experiment. For example, the Cl-Cl bond distance is 3.693 Å, which underestimates the experimental values by ~0.1 Å.

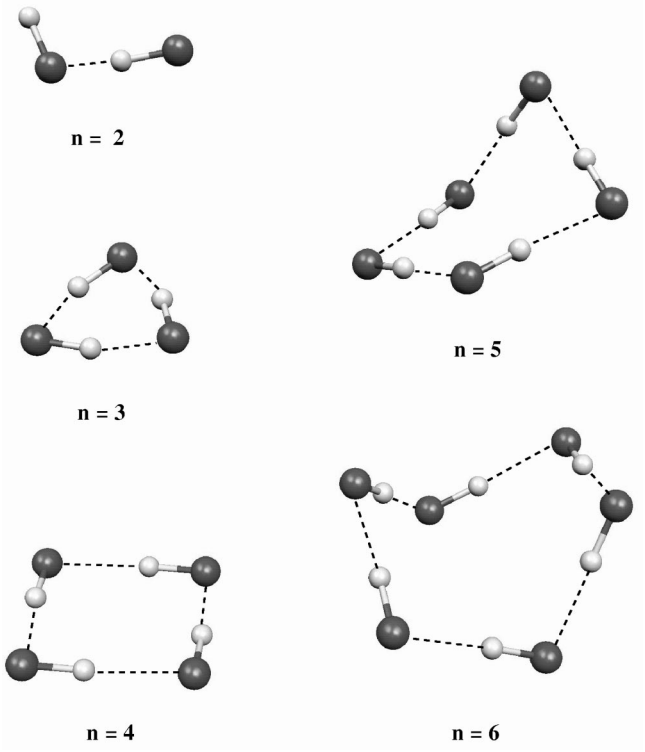

FIG. 3. Optimized structures of $(HCl)_{2-6}$ clusters.

TABLE III. Structural properties of $(HCl)_{2-6}$ clusters. Distances in ångstroms. Angles in degrees.

	$(HCl)_2$	$(HCl)_3$	$(HCl)_4$	$(HCl)_5$	$(HCl)_6$
B3LYP/aug-cc-pVDZ					
H-Cl	1.296	1.307	1.313	1.313	1.313
ClH···Cl	2.537	2.410	2.336	2.326	2.324
Cl-Cl	3.830	3.650	3.646	3.638	3.636
Cl–H–Cl	173.7	157.2	175.2	177.8	178.6
B3PW91/aug-cc-pVDZ					
H-Cl	1.299	1.307	1.314	1.313	1.315
ClH···Cl	2.552	2.475	2.336	2.326	2.258
Cl-Cl	3.850	3.712	3.638	3.580	3.573
Cl–H–Cl	174.4	156.8	175.6	177.8	178.4
MPW1PW91/aug-cc-pVDZ					
H-Cl	1.294	1.305	1.312		1.312
ClH···Cl	2.499	2.392	2.257		2.224
Cl-Cl	3.790	3.630	3.566		3.556
Cl–H–Cl	173.1	157.1	175.6		178.9
Experiment					
Cl-Cl	3.746;[a] 3.797[b]				

[a]From Elrod and Saykally (Ref. 14).
[b]From Ohashi and Pine (Ref. 9).

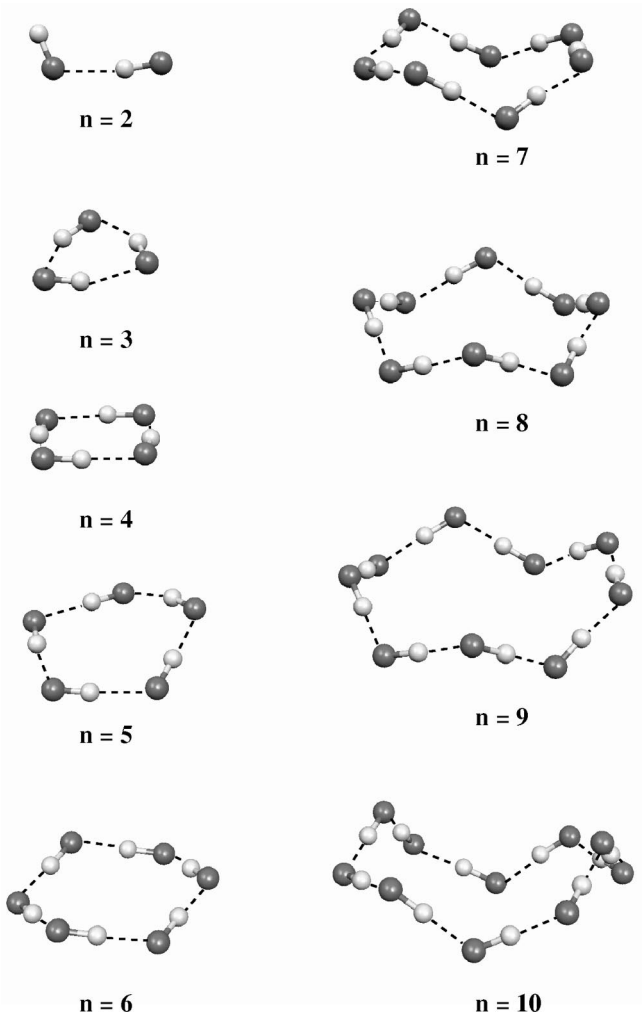

FIG. 4. Optimized structures of $(HF)_{2-10}$ clusters.

Some significant structural changes occur when we move from the HCl dimer to larger HCl clusters. The average Cl-Cl internuclear distance is reduced by ~6% from $(HCl)_2$ to $(HCl)_4$ and then seems to reach a nearly constant value (~3.6 Å) for larger clusters. A quite similar behavior can be observed in the ClH···Cl hydrogen bond. At the MPW1PW1 level it is 2.499 Å in the dimer and 2.224 Å in the pentamer, which means a 12% reduction. With the exception of the $(HCl)_3$ cyclic structure, the average ∠Cl-H-Cl angle shows a tendency to linearity in larger HCl clusters. For example, at the B3LYP/aug-cc-pVDZ level, ∠Cl-H-Cl increases from 175.2° in $(HCl)_4$ to 178.6° in $(HCl)_6$. For the cyclic structures, as the cluster size *n* increases, the need for the H bonds to become nonlinear and be able to support high angular strains diminishes.[8] Deviations from linearity in HCl can be related to the competition between dipolar interactions (that favor linear arrangements) and quadrupolar interactions (favoring perpendicular configurations). The structure of HCl clusters clearly indicate that cooperative effects are very important. In agreement with the behavior of binding energies, these effects increase significantly from the dimer to the tetramer and apparently reach a limit in the hexamer.

The optimized structures of the $(HF)_{2-10}$ clusters are presented in Fig. 4 and some structural parameters are reported in Table IV. The internuclear F-F distance in $(HF)_2$ is 2.723 Å at the MPW1PW91/aug-cc-pVDZ level, in excellent agreement with the experimental value (2.72±0.03 Å).[27] B3LYP and B3PW91 results for F-F (2.730 Å) are also in good agreement with experiment. At the MPW1PW91 level the average F-F distance decreases from 2.723 Å in $(HCl)_2$ to 2.444 Å in $(HCl)_8$, which means a 11% reduction. A similar behavior can be observed for the average HF···H hydrogen bond. It is reduced from 1.804 Å in $(HF)_2$ to 1.479 Å in $(HF)_8$, which is a 22% reduction. The average ∠F-H-F

TABLE IV. Structural properties of $(HF)_{2-10}$ clusters. Distances in ångstroms. Angles in degrees.

	$(HF)_2$	$(HF)_3$	$(HF)_4$	$(HF)_5$	$(HF)_6$	$(HF)_7$	$(HF)_8$	$(HF)_9$	$(HF)_{10}$
B3LYP/aug-cc-pVDZ									
H–F	0.932	0.947	0.961	0.966	0.967	0.967	0.968	0.968	0.968
HF···H	1.806	1.737	1.569	1.519	1.506	1.502	1.500	1.500	1.499
F–F	2.730	2.586	2.509	2.482	2.455	2.452	2.449	2.449	2.449
F–H–F	170.2	147.6	165.0	174.4	178.5	178.4	178.5	178.6	178.6
B3PW91/aug-cc-pVDZ									
H–F	0.932	0.947	0.961	0.966	0.968	0.969	0.969	0.969	0.969
HF···H	1.806	1.806	1.569	1.520	1.487	1.483	1.480	1.480	1.480
F–F	2.730	2.586	2.509	2.482	2.455	2.452	2.449	2.449	2.449
F–H–F	170.2	147.6	165.0	174.4	178.0	178.4	178.6	178.6	178.7
MPW1PW91/aug-cc-pVDZ									
H–F	0.927	0.943	0.958	0.963	0.964	0.965	0.965	0.965	0.965
HF···H	1.804	1.712	1.548	1.499	1.487	1.482	1.479	1.479	1.479
F–F	2.723	2.561	2.487	2.459	2.451	2.447	2.444	2.444	2.444
F–H–F	169.8	147.9	165.3	174.6	177.8	178.3	178.5	178.6	178.6
B3LYP/6-31++G(*d*,*p*)[a]									
HF···H	1.810	1.744	1.562	1.496	1.477	1.474	1.476		
F–F	2.732	2.601	2.500	2.463	2.449	2.445	2.445		
F–H–F	175.9	145.0	162.9	172.6	178.5	182.3	185.0		
Experiment									
F-F	2.72±0.03[b]								

[a]From Rincón *et al.* (Ref. 35).
[b]From Howard *et al.* (Ref. 27).

TABLE V. H-Cl stretching frequencies and average frequency shift relative to the monomer ($\Delta\nu$ in cm^{-1}) in HCl clusters.

	HCl	$(HCl)_2$	$(HCl)_3$	$(HCl)_4$	$(HCl)_5$	$(HCl)_6$
B3PW91/aug-cc-pVDZ						
ν_1	2947	2934	2773	2697	2693	2694
ν_2		2851	2773	2671	2689	2686
ν_3			2722	2671	2653	2680
ν_4				2597	2652	2642
ν_5					2591	2638
ν_6						2590
$\langle\nu\rangle$		2892	2756	2659	2656	2655
$\Delta\nu$		55	191	288	291	292
MPW1PW91/aug-cc-pVDZ						
ν_1	2971	2957	2795	2721		2714
ν_2		2870	2794	2695		2706
ν_3			2743	2695		2701
ν_4				2621		2660
ν_5						2658
ν_6						2609
$\langle\nu\rangle$		2913	2778	2683		2674
$\Delta\nu$		58	193	288		297
MP2/PS+VP^S(2d)^S [a]						
ν_1	3095	3078	3009	2984		
ν_2		3042	3009	2968		
ν_3			2979	2968		
ν_4				2931		
$\langle\nu\rangle$		3060	2999	2963		
$\Delta\nu$		35	96	132		
Experimental		HCl[b]	$(HCl)_2$[c]	$(HCl)_3$[c]	$(HCl)_4$[c]	
ν_1	2889	2856	2787	2763		
ν_2		2818	2787	2748		
ν_3			2760	2748		
ν_4				2716		
$\langle\nu\rangle$		2837	2778	2743		
$\Delta\nu$		52	111	146		

[a]Latajka and Scheiner (Ref. 8).
[b]$(HCl)_n$ in solid Ne (Ref. 15).
[c]$(HCl)_n$ in solid Ar (Ref. 17).

angle exhibits a tendency to linearity in larger HF clusters. At the B3LYP/aug-cc-pVDZ level, $\angle$F-H-F increases from 165° in $(HF)_4$ to 178.5° in $(HF)_6$, and then it is nearly constant in the larger clusters. Table IV also reports B3LYP/6-31++G(d,p) results for $(HF)_{2-8}$ clusters from a recent study by Rincón *et al.*,[35] which are in very good agreement with our B3LYP calculations.

Our results strongly suggest that cooperative effects induced by hydrogen bond are important in both HCl and HF clusters. They also provide some evidence that these effects seem to reach a limit for a relatively small number of monomers (eight in the case of HF). In addition, our results also show that the magnitude of these effects is more important for HF than for HCl clusters.

IV. VIBRATIONAL SHIFT AND ELECTRONIC DENSITY DIFFERENCE

A. Vibrational shift in HCl and HF clusters

Spectroscopic studies of hydrogen halide clusters are frequently carried out in condensed phases, usually inert gas matrices. Interactions with the matrix atoms may influence

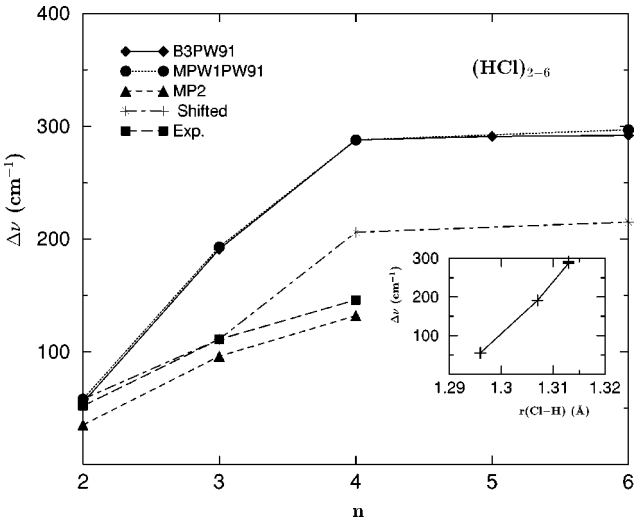

FIG. 5. Average frequency shift $\Delta\nu$ (in cm^{-1}) vs the cluster size n in $(HCl)_{1-6}$ clusters. The inset shows $\Delta\nu$ vs the average Cl-H distance (in Å). DFT optimizations were carried out with the aug-cc-pVDZ basis set. The shifted curve corresponds to a shift of 82 cm^{-1} in the monomer and dimer frequencies. The MP2 curve is based on the $(HCl)_{1-4}$ frequencies from Latajka and Scheiner (Ref. 8).

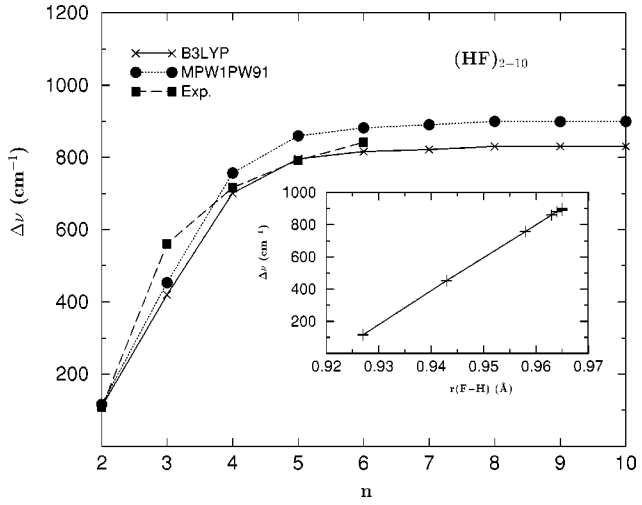

FIG. 6. Average frequency shift $\Delta\nu$ (in cm^{-1}) vs the cluster size in $(HF)_{1-10}$ clusters. The inset shows $\Delta\nu$ vs the average F-H distance (in Å). The experimental curve has been derived from the frequencies reported by Andrews *et al.* (Ref. 29).

the vibrational structure of the hydrogen-bonded complex.[29] There is also theoretical evidence supporting that these interactions modify the shape of the intramolecular potential associated with the guest vibrational motion.[53]

We define the average frequency shift $\Delta\nu$ for each cluster as the difference between the average stretching frequency H-X (X=Cl,F) of the cluster $\langle\nu\rangle$ and the frequency of the monomer. Table V reports $\Delta\nu$'s and frequencies for the HCl clusters. DFT frequencies were not scaled. Some authors[54,55] suggested that DFT zero-point energies should be scaled. However, the empirical scale factor depends on the specific theoretical level.

Harmonic frequencies for HCl and $(HCl)_2$ are higher than experimental values. At the MPW1PW91 level the deviations from experiment are 82 cm^{-1} (HCl) and 76 cm^{-1} for $(HCl)_2$. This is possibly related to the neglect of anharmonicity for the isolated species.[8] For $(HCl)_3$ theoretical frequencies are in very good agreement with experiment. However, for large clusters, gas phase frequencies are lower than experimental values in solid argon.[17] It is possible that condensed phase effects are more important for larger clusters. This could explain the deviation of $\Delta\nu$ from experiment that is illustrated in Fig. 5. We remark that if the theoretical harmonic frequencies of the monomer and dimer are shifted by δ=82 cm^{-1} to correct for anharmonicity, a better agreement with experiment is observed (see Fig. 5). In Table V we also present $\Delta\nu$'s based on frequency calculations by Latajka and Scheiner[8] at the MP2 level with pseudopotential plus valence polarization functions MP2/PS+$VP^S(2d)^S$ level. Good agreement with experiment, which is slightly improved for larger clusters, can be observed (see also Fig. 5). Our results for larger HCl clusters also indicate, in agreement with the results for the binding energies and structural properties, that

TABLE VI. H-F stretching frequencies and average frequency shift relative to the monomer ($\Delta\nu$ in cm^{-1}) in HF clusters.

	HF	$(HF)_2$	$(HF)_3$	$(HF)_4$	$(HF)_5$	$(HF)_6$	$(HF)_7$	$(HF)_8$	$(HF)_9$	$(HF)_{10}$
B3LYP/aug-cc-pVDZ										
ν_1	4059	4016	3686	3481	3393	3395	3384	3389	3383	3386
ν_2		3882	3686	3396	3392	3350	3382	3357	3381	3371
ν_3			3546	3395	3258	3349	3311	3357	3338	3368
ν_4				3163	3257	3195	3310	3271	3333	3317
ν_5					3014	3195	3157	3270	3243	3308
ν_6						2978	3148	3118	3241	3222
ν_7							2967	3117	3100	3211
ν_8								2955	3091	3076
ν_9									2954	3076
ν_{10}										2953
$\langle\nu\rangle$		3949	3639	3358	3263	3243	3237	3229	3229	3229
$\Delta\nu$		110	420	701	796	816	822	830	830	830
MPW1PW91/aug-cc-pVDZ										
ν_1	4129	4084	3726	3503	3408	3410	3397	3401	3395	3397
ν_2		3943	3726	3412	3407	3360	3396	3367	3393	3382
ν_3			3577	3412	3264	3360	3319	3366	3347	3379
ν_4				3164	3263	3195	3317	3274	3341	3324
ν_5					3002	3195	3154	3274	3245	3313
ν_6						2964	3144	3110	3243	3222
ν_7							2950	3109	3091	3210
ν_8								2935	3081	3066
ν_9									2935	3065
ν_{10}										2933
$\langle\nu\rangle$		4013	3676	3372	3269	3247	3239	3229	3230	3229
$\Delta\nu$		116	453	757	860	882	890	900	899	900
Experiment[a]										
$\langle\nu\rangle$	3992	3884	3431	3276	3200	3150	3239			
$\Delta\nu$		108	561	716	792	842				

[a]$(HF)_n$ in solid Ne (Ref. 29).

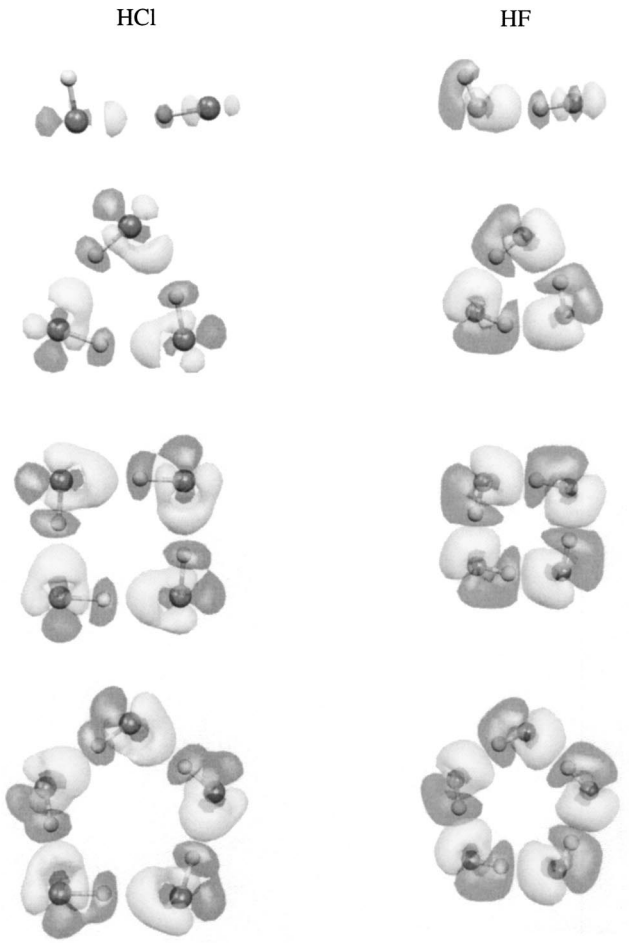

FIG. 7. Electronic density difference $\rho_{D,n}(r)$ in the clusters. The isosurfaces correspond to electronic density differences of $-0.001\,e\,\text{Å}^{-3}$ (dark) and $+0.001\,e\,\text{Å}^{-3}$ (white). Some maxima of $\rho_{D,n}(r)$ (in $e\,\text{Å}^{-3}$) for clusters of size n are (a) HCl 0.04 ($n=2$), 0.08 ($n=3$), 0.11 ($n=4$), 0.12 ($n=5$), 0.11 ($n=6$); (b) HF 0.03 ($n=2$), 0.07 ($n=3$), 0.10 ($n=4$), 0.08 ($n=5$), 0.12 ($n=6$), 0.12 ($n=7$), 0.12 ($n=8$).

hydrogen-bond cooperativity increases from $(HCl)_2$ to $(HCl)_4$, but seems to reach a limit for larger clusters. This is illustrated in Fig. 6, which shows $\Delta\nu$ versus the cluster size n. The inset shows the linear correlation between $\Delta\nu$ and the average H-Cl bond distance in the clusters. Table VI reports $\Delta\nu$'s and frequencies for the HF clusters.

For $(HF)_2$ our results are in very good agreement with experiment.[29] For example, $\Delta\nu=110\ \text{cm}^{-1}$ (B3LYP/aug-cc-pVDZ), in excellent agreement with the experimental value ($108\ \text{cm}^{-1}$). $\Delta\nu$'s for $(HF)_3$ seem to be underestimated by theory. However, for larger clusters a good agreement with experiment is observed. Fig. 6 shows the behavior of $\Delta\nu$ as a function of n for $(HF)_{2-10}$. The inset illustrates the linear correlation between $\Delta\nu$ and the average F-H bond distance. The present results for $\Delta\nu$ in HCl and HF clusters provide a clear illustration of hydrogen-bonding cooperativity that complements the data for binding energies and structure.

B. Electronic density difference

The electronic density reorganization in the clusters, induced by hydrogen bonding, can be analyzed by introducing the electronic density difference $\rho_D(r)$,[56] which is calculated from the electronic density $\rho(r)$. For a cluster of size n, $\rho_{D,n}(r)$ can be defined as:

$$\rho_{D,n}(r)=\rho_n(r)-\sum_{k=1}^{n}\rho_k(r), \tag{3}$$

where $\rho_n(r)$ is the density associated with a cluster with n monomers and the sum involves the electronic density of the monomers in the equilibrium geometry of the cluster.

We have selected isosurfaces corresponding to a total electronic density difference of $-0.001\,e\,\text{Å}^{-3}$ (dark) and $+0.001\,e\,\text{Å}^{-3}$ (white). The isosurfaces are shown in Fig. 7. They suggest a significant electronic density reorganization, which increases from the dimer to the tetramer but seems to be stabilized in larger clusters. This conclusion is also supported by the maxima values of $\rho_{D,n}(r)$, which are reported in the caption of Fig. 7 for the different clusters. For HF they increase from the dimer ($0.03\,e\,\text{Å}^{-3}$) to the pentamer ($0.08\,e\,\text{Å}^{-3}$) and apparently reach a limit ($0.12\,e\,\text{Å}^{-3}$) in the larger clusters. The reorganization is characterized by a shift of electronic density from hydrogen to halide atoms. In particular, the density associated with the central hydrogen of the $XH\cdots X$ bond ($X=$Cl,F) is shifted to the proton acceptor. However, $\rho_{D,n}(r)$ also indicates that the redistribution of the electron density involves the entire cluster.

Comparison between HCl and HF clusters shows a more important electronic density redistribution in the HF dimer and trimer. The results for $\rho_{D,n}(r)$ suggest that hydrogen-bond cooperativity can be also related to the redistribution of the electronic density in the clusters.

V. CONCLUSIONS

This work reports theoretical results for the binding energies, geometries, and vibrational spectra of $(HCl)_{2-6}$ and $(HF)_{2-10}$ clusters. The results are based on density functional theory. Geometry optimizations have been carried out with hybrid functionals. For HF clusters a good agreement with experimental results for the energetics, strucure and vibrational spectrum has been observed. Hybrid functionals (B3LYP, B3PW91, and MPW1PW91) seem to underestimate the $(HCl)_2$ binding energy. Our best result for the dimer binding energy (MPW1PW91/aug-cc-pVQZ) is $-5.9\ \text{kJ mol}^{-1}$, which is $3.6\ \text{kJ mol}^{-1}$ above the experimental result reported by Pine and Howard.[10] This discrepancy seems to reflect the fact that dispersion interactions, which are determined by polarization and correlation effects, are not adequately taken into account by the present set of hybrid functionals.[52] By carrying out single-point energy calculations for HCl clusters with the Perdew and Wang exchange and correlation functional (PW91), the HCl dimer binding energy is in very good agreement with experiment. We have also verified that for the HF dimer the PW91 binding energy is in good agreement with experiment. However, for larger clusters, PW91 binding energies are apparently overestimated.

Our results illustrate the importance of hydrogen-bond (HB) cooperativity in the determination of the energetics, structure, and vibrational properties of HCl and HF clusters.

In addition, we are also providing some evidence that these nonadditive effects levels off for moderately sized clusters ($n=8$ for HCl). This conclusion is supported by the analysis of the dependence on the cluster size of energetical, structural, and vibrational properties.

We have analyzed the behavior of the average frequency shift $\Delta\nu$ as a function of the cluster size. Good agreement with experimental results for HF clusters in solid neon has been observed. For HCl clusters some discrepancies with experiment were observed, mainly for larger clusters. We are also reporting results for electronic density differences in HCl and HF clusters, which illustrate the reorganization of the electronic density induced by hydrogen bonding.

ACKNOWLEDGMENTS

R.C.G. and P.C.d.C. gratefully acknowledge the support of the Fundação para a Ciência e a Tecnologia (FCT) through a Ph.D. Grant (PRAXIS/XXI/BD/15920/98 and PRAXIS/XXI/BD/6503/2001). This work was partially supported by the Sapiens program of the FCT, Portugal (Grant No. POCTI/43315/QUI/2001).

[1] S. Scheiner, *Hydrogen Bonding: A Theoretical Perspective* (Oxford University Press, New York, 1997).
[2] *Theoretical Treatment of Hydrogen Bonding*, edited by Dušan Hadži (Wiley, New York, 1997).
[3] B. F. King and F. Weinhold, J. Chem. Phys. **103**, 333 (1995).
[4] U. C. Singh and P. A. Kollman, J. Comput. Chem. **5**, 129 (1994).
[5] A. J. Stone, A. D. Buckingham, and P. W. Fowler, J. Chem. Phys. **107**, 1030 (1997).
[6] E. D. Isaacs, A. Shukla, P. M. Platzman, D. R. Hamanni, B. Barbielini, and C. A. Tulk, Phys. Rev. Lett. **82**, 600 (1999).
[7] F.-M. Tao and W. Klemperer, J. Chem. Phys. **103**, 950 (1995).
[8] Z. Latajka and S. Scheiner, Chem. Phys. **216**, 37 (1997).
[9] N. Ohashi and A. S. Pine, J. Chem. Phys. **81**, 73 (1984).
[10] A. S. Pine and B. J. Howard, J. Chem. Phys. **84**, 590 (1986).
[11] G. A. Blake, K. L. Busarow, R. C. Cohen, K. B. Laughlin, Y. T. Lee, and R. J. Saykally, J. Chem. Phys. **89**, 6577 (1988).
[12] G. Chalasiński, S. M. Cybulski, M. M. Szcześniak, and S. Scheiner, J. Chem. Phys. **91**, 7048 (1989).
[13] M. D. Schuder, C. M. Lovejoy, R. Nascola, and D. J. Nesbitt, J. Chem. Phys. **99**, 4346 (1993).
[14] M. J. Elrod and R. J. Saykally, J. Chem. Phys. **103**, 921 (1995).
[15] L. Andrews and R. B. Bohn, J. Chem. Phys. **90**, 5205 (1989).
[16] A. Anderson, H. A. Gebbie, and S. H. Walmsley, Mol. Phys. **7**, 401 (1964).
[17] D. Maillard, A. Schriver, J. P. Perchard, C. Girardet, and D. Robert, J. Chem. Phys. **67**, 3917 (1977).
[18] B. J. van der Veken and F. R. de Munck, J. Chem. Phys. **97**, 3060 (1992).
[19] T. Häber, U. Schmitt, and M. A. Suhm, Phys. Chem. Chem. Phys. **1**, 5573 (1999).
[20] J. G. Powles and M. Wojcik, J. Chem. Phys. **78**, 5277 (1983).
[21] A. Karfen, P. R. Bunker, and P. Jensen, Chem. Phys. **149**, 299 (1991).
[22] H. Guo, S. Sirois, E. I. Poroynov, and D. R. Salahub, in *Theoretical Treatment of Hydrogen Bonding*, edited by Dušan Hadži (Wiley, New York, 1997).
[23] J. M. Hermida-Ramón, O. Engkvist, and G. Karlström, J. Comput. Chem. **19**, 1816 (1998).
[24] K. N. Rankin and R. J. Boyd, J. Comput. Chem. **22**, 1590 (2001).
[25] W. D. Chandler, K. E. Johnson, B. D. Fahlman, and J. L. Campbell, Inorg. Chem. **36**, 776 (1997).
[26] J. Janzen and L. S. Bartell, J. Chem. Phys. **50**, 3611 (1969).
[27] B. J. Howard, T. R. Dyke, and W. Klemperer, J. Chem. Phys. **81**, 5417 (1984).
[28] A. S. Pine and W. J. Lafferty, J. Chem. Phys. **78**, 2154 (1983).
[29] L. Andrews, V. E. Bondybev, and J. H. English, J. Chem. Phys. **81**, 3452 (1984).
[30] D. W. Michael and J. M. Lisy, J. Chem. Phys. **85**, 2528 (1986).
[31] S. B. Hendricks, O. Wulf, G. E. Hilbert, and U. Liddell, J. Am. Chem. Soc. **58**, 1936 (1991).
[32] J. E. del Bene, W. B. Person, and K. Szczepaniak, J. Phys. Chem. **99**, 10705 (1995).
[33] S. Hirata and S. Iwata, J. Phys. Chem. A **43**, 8426 (1998).
[34] A. Halkier, W. Klopper, T. Helgaker, P. Jørgensen, and P. R. Taylor, J. Chem. Phys. **111**, 9157 (1999).
[35] L. Rincón, R. Almeida, D. García-Aldea, and H. Diez y Riega, J. Chem. Phys. **114**, 5552 (2001).
[36] M. Quack, U. Schmitt, and M. A. Suhm, Chem. Phys. Lett. **208**, 446 (1993).
[37] L. A. Curtis and M. Blander, Chem. Rev. **88**, 827 (1988).
[38] M. P. Hodges, A. J. Stone, and E. C. Lago, J. Phys. Chem. A **102**, 2455 (1998).
[39] J. F. Gaw, Y. Yamaguchi, M. A. Vincent, and H. F. Schaeffer III, J. Am. Chem. Soc. **106**, 3133 (1984).
[40] A. D. Becke, J. Chem. Phys. **98**, 5648 (1993).
[41] J. P. Perdew and Y. Wang, Phys. Rev. B **45**, 13244 (1992).
[42] C. Lee, W. Yang, and R. G. Parr, Phys. Rev. B **37**, 785 (1988).
[43] C. Adamo and V. Barone, Chem. Phys. Lett. **274**, 242 (1997).
[44] C. Adamo and V. Barone, J. Comput. Chem. **19**, 419 (1998).
[45] C. Adamo and V. Barone, J. Chem. Phys. **108**, 664 (1998).
[46] D. E. Woon and T. H. Dunning, Jr., J. Chem. Phys. **98**, 1358 (1993).
[47] R. A. Kendall, T. H. Dunning, Jr., and R. J. Harrisson, J. Chem. Phys. **96**, 6796 (1992).
[48] M. J. Frisch, G. W. Trucks, H. B. Schlegel *et al.*, GAUSSIAN 98 Gaussian Inc., Pittsburgh, PA, 1998.
[49] S. F. Boys and F. Bernardi, Mol. Phys. **19**, 553 (1970).
[50] S. S. Xantheas, J. Chem. Phys. **104**, 8821 (1986).
[51] A. E. Reed, L. A. Curtiss, and F. Weinhold, Chem. Rev. **88**, 899 (1988).
[52] S. Tsuzuki and H. P. Lüthi, J. Chem. Phys. **114**, 3949 (2001).
[53] J. P. Prates Ramalho, B. J. Costa Cabral, and F. M. S. Silva Fernandes, Chem. Phys. Lett. **184**, 53 (1991).
[54] L. A. Curtiss, K. Raghavachari, P. C. Redfern, and J. A. Pople, Chem. Phys. Lett. **270**, 419 (1997).
[55] C. W. Bauschlicher, Jr., Chem. Phys. Lett. **246**, 40 (1995).
[56] W. H. E. Schwarz, K. Ruedenberg, and L. Mensching, J. Am. Chem. Soc. **111**, 6926 (1989).